

Relativistic Time-of-Arrival and Traversal Time

Andreas Ruschhaupt

Faculty of Physics, University of Bielefeld, Universitätsstr. 25,
D-33615 Bielefeld, Germany

E-mail: rushha@physik.uni-bielefeld.de

Abstract. We compute in a relativistic way the time-of-arrival and the traversal time through a region of a free particle with spin $\frac{1}{2}$. We do this by applying the relativistic extension of the Event-Enhanced Quantum Theory which we have presented in a previous paper. We find a very good coincidence of the results of our formalism and the results obtained by using classical relativistic mechanics.

PACS numbers: 03.65.Xp, 03.65.Pm, 03.65.-w

1. Introduction

Blanchard and Jadczyk [1, 2, 3] have proposed an extension of standard (non-relativistic) quantum mechanics called Event-Enhanced Quantum Theory (EEQT) which main idea is to view the total system as consisting of coupled classical and quantum part. The pure states of the quantum part are wave functions which are not directly observable, whereas the pure states of the classical part can be observed without disturbing them. Changes of the classical pure states are discrete and irreversible, they are called events. A review about applications of EEQT is for example [4].

Blanchard and Jadczyk have also introduced a relativistic extension of EEQT [5] using the idea of a proper time and an indefinite scalar product.

In a previous paper [6], we have presented an alternative approach for a relativistic extension of EEQT. We summarize this approach in Section 2.

The question when a particle arrives at a given point cannot be answered unambiguously in the standard formulation of quantum mechanics. Nevertheless, there exists a lot of approaches to answer the question of “time-of-arrival”. A review about “time-of-arrival” can be for example found in Muga, Sala, and Palao [7] and an extensive review including a lot of references is Muga and Leavens [8].

In this paper, we consider a two dimensional spacetime. We examine the following operational definition of the time-of-arrival: The particle is prepared in a space-time point $(0, x_0)$ and moves freely (except of the influence exerted on it by the detector) in positive x direction. A detector is put at x_D with $x_D > x_0$. It measures the time-of-arrival of the particle at x_D . Because it is possible that the particle is never detected, the experiment or simulation should be stopped after a reasonable and finite period of time.

This definition of time-of-arrival has been examined in the framework of non-relativistic EEQT [9]. In Section 4 of this paper, we will compute the time-of-arrival

using our relativistic extension of EEQT and we will compare the results to those obtained by using classical relativistic mechanics of a point particle.

The question how long a particle needs to traverse a given finite region cannot also be answered unambiguously in the standard formulation of quantum mechanics. This time is called traversal time. It is often examined if a potential is in the given region and the particle must tunnel through the region. Reviews about “traversal time” and “tunnelling time” including a lot of references are for example [10, 11, 12, 13].

“Tunnelling time” has been also examined using the non-relativistic EEQT [14, 15, 16].

In Section 5 of this paper, we examine the “free traversal time” for an always freely moving particle (again except of the influence exerted on the particle by the detectors).

Using two detectors at rest one behind the other, we can measure the traversal time through the region located between the two detectors: The particle is again prepared in a space-time point $(0, x_0)$ and moves in positive x -direction. We put a detector D_1 at x_1 with $x_1 > x_0$. This detector can detect the particle without destroying it. A second detector D_2 is put at x_2 with $x_2 > x_1$. It destroys the particle after detection.

At the beginning of the measurement, both detectors D_1 and D_2 are active. If detector D_1 detects the particle (without destroying it), it turns itself off, but detector D_2 stays turned on. If detector D_2 detects the particle, the experiment is finished.

Thus, the particle can be detected by detector D_1 at a time t_1 and then by detector D_2 at a time t_2 . If this happens, the time difference $t_2 - t_1$ is defined to be the “traversal time”.

It is also possible that the particle is detected by D_2 without prior detection by D_1 , but this situation should not contribute to traversal times.

Moreover, it is possible that the particle is never detected or only detected one time by detector D_1 . For this reason the experiment or simulation should be stopped after a reasonable and finite period of time.

We will compute the traversal time using our relativistic extension of EEQT. Again we will compare the results to those obtained using classical relativistic mechanics of a point particle.

2. A Relativistic Extension of EEQT

We recall the extension of EEQT which we have proposed in [6]. It describes one spin $\frac{1}{2}$ -particle in a relativistic way and in four dimensional spacetime. Here, we restrict ourself to consider two dimensional spacetime.

As in EEQT, we postulate that the total system consists of a classical and a quantum part which are coupled. Because of that, at a given proper time τ , the (pure) state of the total system is a pair (ω_τ, Ψ_τ) . ω_τ is the state of the classical part and Ψ_τ is the state of the quantum part.

We assume that a (pure) state ω_τ of the classical part is a number: $\omega_\tau \in \mathbb{N}_0 = \{0, 1, 2, \dots\}$. We also call a change of the classical (pure) state “event” as in non-relativistic EEQT.

The (pure) states of the quantum part shall be (heuristically) solutions $\Psi : \mathbb{R} \times \mathbb{R} \rightarrow \mathbb{C}^4$ of the Dirac equation. Because we examine only free particles in this

paper, we use the free Dirac equation:

$$i\hbar c \frac{\partial}{\partial(ct)} \Psi(ct, x) = H_0 \Psi(ct, x) \quad (1)$$

with $H_0 = -i\hbar\gamma^0\gamma^1\frac{\partial}{\partial x} + mc^2\gamma^0$. We denote the space of quantum states by \mathcal{H} . A more precise definition of \mathcal{H} can be found in [6]. We use the Dirac or standard representation of the γ -matrices. Let $\mathcal{P} = \{(y^0, y^1, \alpha) : y^0, y^1, \alpha \in \mathbb{R}, |\alpha| < 1\}$ and $\sigma_\lambda(u) = (y^0 + \alpha \cdot u, y^1 + u)$, $\forall u \in \mathbb{R}, \forall \lambda \equiv (y^0, y^1, \alpha) \in \mathcal{P}$. We now introduce a positive-definite scalar product between two quantum states $\Psi_A, \Psi_B \in \mathcal{H}$:

$$\langle \Psi_A | \Psi_B \rangle_{\mathcal{H}} := \int_{\sigma_\lambda} j_{AB}^\mu df_\mu \quad (2)$$

with $\lambda \in \mathcal{P}$, $j_{AB}^\mu = \Psi_A^+ \gamma^0 \gamma^\mu \Psi_B$ and $df_\mu = (1, -\alpha) du$ denotes the differential ‘‘surface’’ element of σ_λ . This scalar product is well defined because it is independent of λ . This follows from Gauss theorem and the fact that $\partial_\mu j_{AB}^\mu = 0$. Moreover, one can show that this scalar product is covariant, its value being independent of the reference frame.

We introduce the operators $U_{(ct_0, x_0)}$ with $ct_0, x_0 \in \mathbb{R}$:

$$(U_{(ct_0, x_0)} \Psi)(x) := \Psi(ct_0, x_0 + x)$$

An interesting property of a quantum state is that it is uniquely given by its values on a space-like hyperplane σ_λ . Therefore, the operators $U_{(ct_0, x_0)}$ are invertible. $\Psi = U_{(ct_0, x_0)}^{-1} \psi$ is the solution of the free Dirac equation (1) fulfilling the initial condition $\Psi(ct_0, x) = \psi(x - x_0)$. We get

$$\Psi(ct, x) = (U_{(ct_0, x_0)}^{-1} \psi)(ct, x) = \exp\left(-\frac{i}{\hbar}(t - t_0)H_0\right) \psi(x - x_0)$$

Now, we want to formulate an algorithm for modelling continuous relativistic measurements, indeed we will propose in the following an algorithm to simulate detections of the particle. In principle, we will do this by rewriting the algorithm of EEQT, replacing t with τ and using our Hilbert space of ‘‘solutions.’’

We denote the reference frame by K . The particle is prepared at proper time τ_0 in a point (ct_0, x_0) .

We consider n detectors with trajectories $z_j(\tau)$, $j = 1..n$. The trajectories start at proper time $\tau = \tau_0$ from the backward light-cone of the space-time point of the ‘‘preparation event’’:

$$(ct_0 - z_j^0(\tau_0))^2 - (x_0 - z_j^1(\tau_0))^2 = 0, \quad z_j^0(\tau_0) \leq ct_0$$

We allow detections which happen in the past of the preparation time. But we do not allow detections, if the detection space-time point is located in the backward light-cone of the space-time point of the preparation event.

Each detector is characterized by operators $G_j(\tau) : \mathcal{H} \rightarrow \mathcal{H}$. Let $G_j^\pm(\tau)$ be the adjoint operator. The total coupling between the quantum and the classical part is given by $\Lambda(\tau) := \sum_{j=1}^n G_j^\pm(\tau) G_j(\tau)$.

We define a detection algorithm in the following way:

- (i) The particle is prepared in a space-time point (ct_0, x_0) at proper time $\tau = \tau_0$. The quantum state is Ψ_{τ_0} with $\|\Psi_{\tau_0}\|_{\mathcal{H}}^2 \equiv \langle \Psi_{\tau_0} | \Psi_{\tau_0} \rangle_{\mathcal{H}} = 1$ and the classical state is $\omega_{\tau_0} = 0$.
- (ii) Choose uniformly a random number $r \in [0, 1]$.

(iii) Propagate the quantum state forward in proper time by solving

$$\frac{\partial}{\partial \tau} \Psi_\tau = -\frac{1}{2} \Lambda(\tau) \Psi_\tau \quad (3)$$

until $\tau = \tau_1$, where τ_1 is defined by

$$1 - \|\Psi_{\tau_1}\|_{\mathcal{H}}^2 = \int_{\tau_0}^{\tau_1} d\tau \langle \Psi_\tau | \Lambda \Psi_\tau \rangle_{\mathcal{H}} = r$$

Let $\omega_\tau = \omega_{\tau_0}$ until $\tau = \tau_1$, a detection happens at proper time $\tau = \tau_1$.

(iv) We choose the detector k - which detects the particle - with probability

$$p_k = \frac{1}{N} \|G_k(\tau_1) \Psi_{\tau_1}\|_{\mathcal{H}}^2$$

with $N = \sum_{j=1}^n \|G_j(\tau_1) \Psi_{\tau_1}\|_{\mathcal{H}}^2$.

(v) Let l be the detector which detects effectively the particle. The detection happens at the point $z_l(\tau_1)$. The detection induces the following change of the states:

$$(\omega_{\tau_1}, \Psi_{\tau_1}) \longrightarrow \left(l, \frac{G_l(\tau_1) \Psi_{\tau_1}}{\|G_l(\tau_1) \Psi_{\tau_1}\|_{\mathcal{H}}} \right)$$

The algorithm can start again perhaps with other detectors at position (ii).

Because the scalar product is covariant, this algorithm is covariant. Moreover, its non-relativistic limit reduces to the algorithm of the non-relativistic EEQT. If we “charge conjugate” the initial state $\Psi_{\tau_0} \rightarrow \Psi_{\tau_0}^C \equiv C \gamma^{0T} \Psi_{\tau_0}^*$ and the detector functions $G_j(\tau) \rightarrow C \gamma^{0T} G_j^*(\tau) \gamma^{0T} C^+$ with $C = i\gamma^2 \gamma^0$, then the algorithm will give the same detections as if we start with Ψ_{τ_0} and $G_j(\tau)$ (if we choose the same random numbers). The quantum state in the “charge conjugated” world Ψ_τ^C and the quantum state in the “normal” world are always connected by $\Psi_\tau^C = C \gamma^{0T} \Psi_\tau^*$.

Note, that we have also formulated an algorithm for modelling ideal measurements of infinitesimal small duration in [6]. It can be seen as playing the role of a relativistic, covariant reduction postulate.

3. Initial quantum state

The particle is prepared at proper time $\tau = \tau_0$ in the space-time point $(0, x_0)$ with a mean momentum p_0 . We examine three different initial states of the particle in this paper. Remember that a initial states of the particle must be a solution of the Dirac equation (1).

The first state corresponds to a state with only positive energies:

$$\Psi_{0,P}(ct, x) = \frac{1}{N_P} \int dk \frac{1}{2\hat{E}} \cdot F_{\Delta k} \left(k - \frac{p_0}{\hbar} \right) \begin{pmatrix} \hat{E} + \hat{m} \\ 0 \\ 0 \\ k \end{pmatrix} \cdot \exp \left(ik(x - x_0) - i\hat{E}ct \right)$$

with $\hat{m} = \frac{mc}{\hbar}$, $\hat{E} = \sqrt{k^2 + \hat{m}^2}$, $\Delta k = 10 \text{ \AA}^{-1}$,

$$F_{\Delta k}(k) = \begin{cases} \exp \left(-\frac{k^2}{\Delta k^2 - k^2} \right) & \text{for } |k| < \Delta k \\ 0 & \text{otherwise} \end{cases}$$

and N_P being a normalization factor so that $\|\Psi_{0,P}\|_{\mathcal{H}}^2 = 1$. This state describes an electron with charge $-e$.

The second one corresponds to a state with only negative energies:

$$\Psi_{0,N}(ct, x) = \frac{1}{N_N} \int dk \frac{1}{2\hat{E}} \cdot F_{\Delta k} \left(k - \frac{p_0}{\hbar} \right) \begin{pmatrix} \hat{E} - \hat{m} \\ 0 \\ 0 \\ k \end{pmatrix} \cdot \exp \left(-ik(x - x_0) + i\hat{E}ct \right)$$

with N_N being a normalization factor so that $\|\Psi_{0,N}\|_{\mathcal{H}}^2 = 1$. Remember that the above algorithm is invariant under charge conjugation. If we consider the charge conjugate of the initial state and the detector functions, we get the same events. Because the “charge conjugated” world and the “normal world” should describe the same physical situation and because the charge conjugation of $\Psi_{0,N}$ describes a particle with charge $+e$ in the “charge conjugated world”, we demand that the initial state $\Psi_{0,N}$ describes a positron with charge $+e$ also in the “normal” world.

As third initial state, we want to use a mixed state:

$$\begin{aligned} \Psi_{0,PN}(ct, x) &= U_{(0,x_0)}^{-1} \left[\frac{1}{(2\pi)^{1/4} \sqrt{\eta}} \cdot \exp \left(-\frac{x^2}{4\eta^2} + i\frac{p_0}{\hbar}x \right) \cdot \begin{pmatrix} 1 \\ 0 \\ 0 \\ 0 \end{pmatrix} \right] (ct, x) \\ &= \frac{\sqrt{2\eta}}{(2\pi)^{3/4}} \int dk \frac{1}{2\hat{E}} \exp \left(-\eta^2 \left(k - \frac{p_0}{\hbar} \right)^2 \right) \begin{pmatrix} \hat{E} + \hat{m} \\ 0 \\ 0 \\ k \end{pmatrix} \cdot \exp \left(ik(x - x_0) - i\hat{E}ct \right) \\ &\quad + \frac{\sqrt{2\eta}}{(2\pi)^{3/4}} \int dk \frac{1}{2\hat{E}} \exp \left(-\eta^2 \left(k + \frac{p_0}{\hbar} \right)^2 \right) \begin{pmatrix} \hat{E} - \hat{m} \\ 0 \\ 0 \\ k \end{pmatrix} \cdot \exp \left(-ik(x - x_0) + i\hat{E}ct \right) \end{aligned}$$

with $\eta = 0.1 \text{ \AA}$. The constants are chosen in such a way that $\|\Psi_{0,PN}\|_{\mathcal{H}}^2 = 1$. The physical interpretation of the mixed state is the following: we assume that the particle (a single particle) can be in an “electron-state” (solution with positive energies) and in a “positron-state” (solution with negative energies), in analogy to the case, that a particle can be e.g. in a spin $+\frac{1}{2}$ -state or in a spin $-\frac{1}{2}$ -state. Superpositions as $\Psi_{0,PN}$ of the two states should be (in analogy to the spin-case) possible and allowed.

4. Free Time-of-Arrival

In this section, we apply the above algorithm to simulate the detection of the particle by one detector which is at rest.

We want to compare the results to those which we obtain by using classical relativistic mechanics of a point-particle.

Let us use the reference frame K_0 in which the detector is at rest. In this reference frame, the particle is prepared at proper time $\tau_0 = 0$ in the space-time point $(0, x_0)$ with a mean momentum p_0 . The detector is put at x_D , its trajectory is $z(\tau) = (c\tau + x_0 - x_D, x_D)$. The coupling operator should be given by

$$G(\tau) = U_{z(\tau)}^{-1} g(x) U_{z(\tau)}$$

with $g(x)$ characterizing the sensitivity of the detector:

$$g(x) = \sqrt{\frac{2W_D}{\hbar}} \cdot F_{\frac{\Delta x_D}{2}}(x)$$

The adjoint operator is $G^+(\tau) = U_{z(\tau)}^{-1} g^+(x) U_{z(\tau)}$.

Because it is possible that the particle is never detected, we stop the algorithm at $\tau = \tau_{CUT}$ (with τ_{CUT} large).

We want to recall that the algorithm is covariant. The choice of K_0 as the reference frame is arbitrary. The algorithm can be applied in any reference frame, and it will result (if we choose the same random numbers) the same events in all reference frames.

Using our algorithm, the probability that the detector detects the particle at all is given by

$$P_\infty = \int_0^{\tau_{CUT}} d\tau \langle \Psi_\tau | \Lambda \Psi_\tau \rangle_{\mathcal{H}}$$

The probability density for a ‘‘proper time-of-arrival’’ at the detector is given by ($\tau < \tau_{CUT}$)

$$p(\tau) = \frac{1}{P_\infty} \langle \Psi_\tau | \Lambda \Psi_\tau \rangle_{\mathcal{H}}$$

It is zero for $\tau \leq 0$ and $\tau \geq \tau_{CUT}$.

Using this probability density for ‘‘proper time-of-arrival’’, we can calculate the probability density and the expectation value for the time-of-arrival in an arbitrary reference frame.

Let us first look at the detector’s rest-frame K_0 . If a detection happens at proper time τ , then it happens in space-time point $z(\tau) = (c\tau + x_0 - x_D, x_D)$. This implies a time-of-arrival of $t = \tau - \frac{x_D - x_0}{c}$. So we get the following probability density for the time-of-arrival in the detector’s rest-frame K_0 :

$$\varrho_0(t) = p\left(t + \frac{x_D - x_0}{c}\right)$$

The expectation value (or mean time-of-arrival) is

$$T_{a,0} = \int dt t \varrho_0(t) = \int d\tau \left(\tau - \frac{x_D - x_0}{c}\right) p(\tau) = \int d\tau \tau p(\tau) - \frac{x_D - x_0}{c}$$

Now, we want to calculate these values in a reference frame K_v which moves with velocity v with respect to the detector’s rest-frame K_0 . The Poincaré-transformation $K_0 \rightarrow K_v$ has the following form:

$$\tilde{x} = \frac{1}{\sqrt{1 - \frac{v^2}{c^2}}} \begin{pmatrix} 1 & -\frac{v}{c} \\ -\frac{v}{c} & 1 \end{pmatrix} x$$

The detector trajectory in K_v is

$$\tilde{z}(\tau) = \left(1 - \frac{v^2}{c^2}\right)^{-\frac{1}{2}} \cdot (c\tau + x_0 - x_D - v/c \cdot x_D, \quad -v\tau - v/c \cdot x_0 + v/c \cdot x_D + x_D)$$

So the normalized probability density for the time-of-arrival in the reference frame K_v is given by

$$\varrho_v(\tilde{t}) = \sqrt{1 - \frac{v^2}{c^2}} \cdot p\left(\sqrt{1 - \frac{v^2}{c^2}} \tilde{t} + \frac{x_D - x_0}{c} + \frac{v}{c^2} x_D\right)$$

and the expectation value (or mean time-of-arrival) in K_v is given by

$$T_{a,v} = \int d\tilde{t} \tilde{t} \varrho_v(\tilde{t}) = \frac{1}{\sqrt{1 - \frac{v^2}{c^2}}} \left[T_{a,0} - \frac{v}{c^2} x_D \right] \quad (4)$$

4.1. Numerical Approach

We use the reference frame K_0 to compute $p(\tau)$. Therefore, we define

$$\Omega(\tau, x) := (U_{z(\tau)}\Psi_\tau)(x) = \Psi_\tau(c\tau + x_0 - x_D, x_D + x)$$

If Ψ_τ is a solution of (1) and (3), then we get

$$\begin{aligned} & i\hbar \frac{\partial}{\partial \tau} \Omega(\tau, x) \\ &= i\hbar c \frac{\partial}{\partial(ct)} \Psi_\tau(\overbrace{c\tau + x_0 - x_D}^{ct}, x_D + x) + i\hbar \left(\frac{\partial \Psi_\tau}{\partial \tau} \right) (c\tau + x_0 - x_D, x_D + x) \\ &= H_0 \Omega(\tau, x) - i \frac{\hbar}{2} g^+(x) g(x) \Omega(\tau, x) \end{aligned} \quad (5)$$

We have to solve this equation with the initial condition $\Omega(0, x) = \Psi_0(x_0 - x_D, x_D + x)$. Using $\langle \Psi_\tau | \Lambda \Psi_\tau \rangle_{\mathcal{H}} = \int dx \Omega^+(\tau, x) g^+(x) g(x) \Omega(\tau, x)$, we can calculate P_∞ and $p(\tau)$ if we know $\Omega(\tau, x)$. Using $p(\tau)$, we get $\varrho_0(t)$ and $T_{a,0}$.

The equation (5) with the initial condition $\Omega(0, x) = \Psi_0(x_0 - x_D, x_D + x)$ is solved numerically. The proper time dynamics of Ω is approximated by

$$\Omega(\tau + \Delta\tau) \approx \exp\left(-\frac{\Delta\tau}{2} \frac{1}{2} g^+(x) g(x)\right) \exp\left(-\Delta\tau \frac{i}{\hbar} H_0\right) \exp\left(-\frac{\Delta\tau}{2} \frac{1}{2} g^+(x) g(x)\right) \Omega(\tau)$$

We now discretize the proper time and the space with steps $\Delta x_B = c\Delta\tau_B = 0.0004 \text{ \AA}$. Then, the first and the last operator can be computed directly. The second operator is discretized by using the method of Wessels, Caspers, and Wiegel [17]. The boundary conditions are walls at $x = -6 \text{ \AA}$ and at $x = 4 \text{ \AA}$ in such a way that $\Omega(\tau, -6 \text{ \AA}) = \Omega(\tau, 4 \text{ \AA}) = 0$ for all τ . We set: $\tau_{CUT} = 13.0 \text{ \AA}/c$ ($p_0 < 0.5 mc$), $\tau_{CUT} = 7.0 \text{ \AA}/c$ ($0.5 mc \leq p_0 < 0.75 mc$), $\tau_{CUT} = 5.0 \text{ \AA}/c$ ($0.75 mc \leq p_0 < 1.0 mc$), $\tau_{CUT} = 4.5 \text{ \AA}/c$ ($1.0 mc \leq p_0$). We do the simulations again with other time and space steps $\Delta x_A = c\Delta\tau_A = 0.0006 \text{ \AA}$. So the error in the expectation value $T_{a,0}$ can be approximated by

$$error(T_{a,0}) = \pm \frac{\Delta x_B}{\Delta x_A - \Delta x_B} |T_{a,0}(\Delta x_B) - T_{a,0}(\Delta x_A)| \quad (6)$$

4.2. Results

We set $x_0 = -1 \text{ \AA}$, $x_D = 0 \text{ \AA}$, $\Delta x_D = 0.01 \text{ \AA}$ and $W_D = 1 \times 10^{-5} mc^2$.

Figure 1 shows the corresponding expectation values of the time-of-arrival $T_{a,0}$ in the detector's rest-frame K_0 for different momenta p_0 and for the three different initial states. The error bars are calculated using (6).

In addition, Figure 1 shows the arrival-times calculated by using the classical relativistic mechanics of a point-particle:

$$t_{a,RM} = \frac{x_D - x_0}{c} \sqrt{1 + \frac{m^2 c^2}{p_0^2}}$$

We see that the expectation values are nearly independent of the initial state $\Psi_{0,PN}$, $\Psi_{0,P}$ or $\Psi_{0,N}$. Furthermore, it exists a good agreement between the values we computed and the results obtained by using classical relativistic mechanics.

Only for very high momenta, the expectation values of the simulation with $\Psi_{0,PN}$ are a bit smaller than the times from classical mechanics and those obtained by the simulations with other initial states.

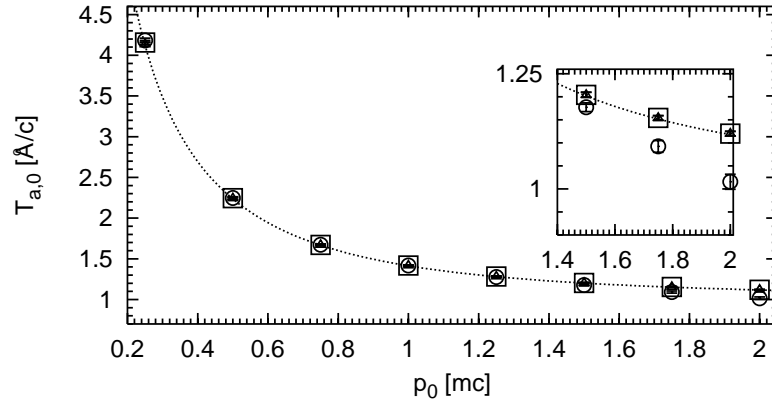


Figure 1. Mean time-of-arrival $T_{a,0}$ versus particle momentum p_0 in the detector’s rest-frame K_0 , relativistic simulation with detector parameters $\Delta x_D = 0.01 \text{ \AA}$, $W_D = 1 \times 10^{-5} mc^2$ started with different initial states : $\Psi_{0,P}$ (boxes with error bars), $\Psi_{0,N}$ (triangles with error bars), $\Psi_{0,PN}$ (circles with error bars), other parameters see text; classical relativistic mechanics $t_{a,RM}$ (dotted line); the figure inside is a zoom of the right lower area of the figure outside

The reason can be seen in Figure 2, which shows probability densities in the detector’s rest-frame K_0 . For very high momenta and if we start with $\Psi_{0,PN}$, we find a small probability for negative times-of-arrival. This fact explains why the expectation values of the simulation with $\Psi_{0,PN}$ are smaller than the results of classical mechanics and those of the other simulations.

We also see that the probability densities are (nearly) the same if we start with $\Psi_{0,P}$ or $\Psi_{0,N}$.

The expectation values $T_{a,v}$ in different reference frames are connected by (4).

We get from classical relativistic mechanics: the time-of-arrival $\tilde{t}_{a,RM}$ in the reference frame K_v is connected to the result $t_{a,RM}$ in the reference frame K_0 in the same manner:

$$\tilde{t}_{a,RM} = \frac{1}{\sqrt{1 - \frac{v^2}{c^2}}} \left[t_{a,RM} - \frac{v}{c^2} x_D \right]$$

So we have a good agreement between the simulated expectation values and the results deduced from classical relativistic mechanics in all reference frames!

Another important and interesting question is how the expectation values depend on the parameters of the detector. The initial state is now the function $\Psi_{0,P}$ with positive energies. We examine those particle momenta which are also examined in Figure 1. We compute the probability densities and the expectation values for four different pairs of detector parameters.

First, we examine the case of a “higher” detector with $W_D = 1.0 mc^2$, but its width is still $\Delta x_D = 0.01 \text{ \AA}$. We find that the expectation values and the normalized probability densities do not change by using a “higher” detector for all examined particle momenta. The detection probability P_∞ increases with increasing detector height W_D .

Next, we examine the case of a wider detector with $\Delta x_D = 0.4 \text{ \AA}$ and $W_D =$

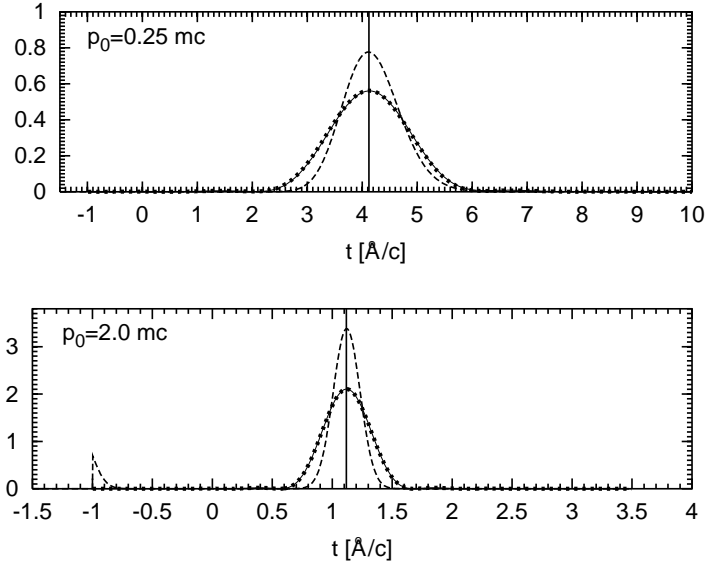


Figure 2. Probability densities ϱ_0 for the time-of-arrival in the detector's rest-frame K_0 , detector parameters: $\Delta x_D = 0.01 \text{ \AA}$, $W_D = 1 \times 10^{-5} mc^2$, initial state: $\Psi_{0,P}$ (small solid line), $\Psi_{0,N}$ (big dotted line), $\Psi_{0,PN}$ (dashed line), particle momentum p_0 ; the vertical solid line indicates the arrival time deduced from classical relativistic mechanics

$1 \times 10^{-5} mc^2$. The expectation values do not change. The normalized probability density do not change in a significant way, it only becomes a bit wider. Again the detection probability P_∞ increases with increasing detector width Δx_D .

The results only change if we use a very wide and height detector with $\Delta x_D = 0.4 \text{ \AA}$ and $W_D = 1.0 mc^2$. The expectation values and the normalized probability densities are then shifted to earlier times.

In other words, the simulations show that it exists a wide range of detector parameters for which the results do not change significantly.

5. Free Traversal Time

In this section, we simulate the traversal time measurement described in Section 1 by applying our algorithm being described in Section 2.

We use the detectors' rest-frame K_0 . The particle is prepared at proper time $\tau_0 = 0$ in $(0, x_0)$. The first detector D_1 is at rest at position x_1 . Its trajectory is $z_1(\tau) = (c\tau + x_0 - x_1, x_1)$. The second detector D_2 is at rest at position x_2 . Its trajectory is $z_2(\tau) = (c\tau + x_0 - x_2, x_2)$. The coupling operators of detector D_j should be given by

$$G_j(\tau) = U_{z_j(\tau)}^{-1} g_j(x) U_{z_j(\tau)} \quad j = 1, 2$$

with $g(x)$ characterizing the sensitivity of the detector D_j :

$$g_j(x) = \sqrt{\frac{2W_j}{\hbar}} \cdot F_{\frac{\Delta x_j}{2}}(x)$$

Because it is possible that the particle is not detected two times, we stop the algorithm at $\tau = \tau_{CUT}$ (with τ_{CUT} large).

Let Ψ_0 be the initial state and Ψ_τ the solution of (1) and (3). Then, the probability that the particle is detected by D_1 at all is

$$P_{\infty,1} = \int_0^{\tau_{CUT}} d\tau \langle \Psi_\tau | G_1^+(\tau) G_1(\tau) \Psi_\tau \rangle_{\mathcal{H}}$$

The probability density that the particle is detected by D_1 is given by ($\tau < \tau_{CUT}$)

$$p_1(\tau) = \frac{1}{P_{\infty,1}} \langle \Psi_\tau | G_1^+(\tau) G_1(\tau) \Psi_\tau \rangle_{\mathcal{H}}$$

If a detection by detector D_1 happens at τ_1 , the quantum state after the detection is given by:

$$\Phi_{\tau_1}^{(\tau_1)} := \frac{G_1(\tau_1) \Psi_{\tau_1}}{\|G_1(\tau_1) \Psi_{\tau_1}\|_{\mathcal{H}}} \quad (7)$$

Let $\Phi_\tau^{(\tau_1)}$ be the solution of (3) with initial state (7). We get the following conditional probability that the particle is detected a second time by D_2 if it is detected by D_1 at τ_1 :

$$P_\infty^{(\tau_1)} = \int_{\tau_1}^{\tau_{CUT}} d\tau_2 \langle \Phi_{\tau_2}^{(\tau_1)} | G_2^+(\tau_2) G_2(\tau_2) \Phi_{\tau_2}^{(\tau_1)} \rangle_{\mathcal{H}}$$

The probability density for a second detection at proper time τ_2 by detector D_2 after a detection of detector D_1 at proper time τ_1 is given by

$$p_2^{(\tau_1)}(\tau_2) = \frac{1}{P_\infty^{(\tau_1)}} \langle \Phi_{\tau_2}^{(\tau_1)} | G_2^+(\tau_2) G_2(\tau_2) \Phi_{\tau_2}^{(\tau_1)} \rangle_{\mathcal{H}}$$

Finally, the probability density for a first detection by D_1 at τ_1 and a second detection by D_2 at τ_2 is

$$\begin{aligned} p_{12}(\tau_1, \tau_2) &= \frac{p_2^{(\tau_1)}(\tau_2) \cdot P_\infty^{(\tau_1)} \cdot p_1(\tau_1) \cdot P_{\infty,1}}{\int_0^{\tau_{CUT}} d\tau P_\infty^{(\tau)} \cdot p_1(\tau) \cdot P_{\infty,1}} \\ &= \frac{1}{P_{\infty,12}} \cdot \begin{cases} \langle \Phi_{\tau_2}^{(\tau_1)} | G_2^+(\tau_2) G_2(\tau_2) \Phi_{\tau_2}^{(\tau_1)} \rangle_{\mathcal{H}} \cdot \langle \Psi_{\tau_1} | G_1^+(\tau_1) G_1(\tau_1) \Psi_{\tau_1} \rangle_{\mathcal{H}} \\ \text{for } 0 < \tau_1 < \tau_{CUT} \text{ and } \tau_1 < \tau_2 < \tau_{CUT} \\ 0 \quad \text{otherwise} \end{cases} \end{aligned}$$

with $P_{\infty,12}$ being the probability that the particle is detected two times:

$$\begin{aligned} P_{\infty,12} &= P_{\infty,1} \cdot \int_0^{\tau_{CUT}} d\tau P_\infty^{(\tau)} \cdot p_1(\tau) \\ &= \int_0^{\tau_{CUT}} d\tau_1 \int_{\tau_1}^{\tau_{CUT}} d\tau_2 \langle \Phi_{\tau_2}^{(\tau_1)} | G_2^+(\tau_2) G_2(\tau_2) \Phi_{\tau_2}^{(\tau_1)} \rangle_{\mathcal{H}} \cdot \langle \Psi_{\tau_1} | G_1^+(\tau_1) G_1(\tau_1) \Psi_{\tau_1} \rangle_{\mathcal{H}} \end{aligned}$$

Note, that this probability density is independent of the reference frame in which the algorithm is applied.

We now calculate traversal times in different reference frames. In contrast to p_{12} , the probability density for traversal time depends on the reference frame.

We start with the detectors' rest-frame K_0 . If the first detection of D_1 happens at proper time τ_1 , then it happens at space-time point $z_1(\tau_1) = (c\tau_1 + x_0 - x_1, x_1)$. If

the second detection of D_2 happens at proper time τ_2 , then it happens at space-time $z_2(\tau_2) = (c\tau_2 + x_0 - x_2, x_2)$. The resulting traversal time is therefore

$$t = \tau_2 + \frac{x_0 - x_2}{c} - \tau_1 - \frac{x_0 - x_1}{c} = \tau_2 - \tau_1 - \frac{x_2 - x_1}{c}$$

So the normalized probability density for the traversal time in the detectors' rest-frame K_0 is given by

$$\rho_0(t) = \int d\tau p_{12} \left(\tau, t + \frac{x_2 - x_1}{c} + \tau \right)$$

The expectation value of the traversal time (or mean traversal time) in K_0 is

$$T_{t,0} = \int dt t \cdot \int d\tau p_{12} \left(\tau, t + \frac{x_2 - x_1}{c} + \tau \right)$$

Now, we want to calculate these values in the reference frame K_v (the reference frame which moves with velocity v with respect to the detectors' rest-frame K_0).

The detector trajectories in K_v are

$$\begin{aligned} \tilde{z}_1(\tau) &= \frac{1}{\sqrt{1 - \frac{v^2}{c^2}}} \cdot \left(c\tau + x_0 - x_1 - \frac{v}{c}x_1, -v\tau - \frac{v}{c}(x_0 - x_1) + x_1 \right) \\ \tilde{z}_2(\tau) &= \frac{1}{\sqrt{1 - \frac{v^2}{c^2}}} \cdot \left(c\tau + x_0 - x_2 - \frac{v}{c}x_2, -v\tau - \frac{v}{c}(x_0 - x_2) + x_2 \right) \end{aligned}$$

If the first detection of D_1 happens at τ_1 and the second detection of D_2 happens at τ_2 , then it results a traversal time of

$$\tilde{t} = \frac{1}{\sqrt{1 - \frac{v^2}{c^2}}} \cdot \left(\tau_2 - \tau_1 - \frac{x_2 - x_1}{c} - \frac{v}{c^2}(x_2 - x_1) \right)$$

So the normalized probability density for the traversal time in the reference frame K_v is given by

$$\rho_v(\tilde{t}) = \sqrt{1 - \frac{v^2}{c^2}} \cdot \int d\tau p_{12} \left(\tau, \sqrt{1 - \frac{v^2}{c^2}} \tilde{t} + \frac{x_2 - x_1}{c} + \frac{v}{c^2}(x_2 - x_1) + \tau \right)$$

The expectation value of the traversal time (or mean traversal time) in K_v is

$$\begin{aligned} T_{t,v} &= \int dt t \cdot \sqrt{1 - \frac{v^2}{c^2}} \cdot \int d\tau p_{12} \left(\tau, \sqrt{1 - \frac{v^2}{c^2}} \tilde{t} + \frac{x_2 - x_1}{c} + \frac{v}{c^2}(x_2 - x_1) + \tau \right) \\ &= \frac{1}{\sqrt{1 - \frac{v^2}{c^2}}} \left[T_{t,0} - \frac{v}{c^2}(x_2 - x_1) \right] \end{aligned} \quad (8)$$

5.1. Numerical Approach

We use the reference frame K_0 . For computation of the algorithm until the first detection, we define

$$\Omega_A(\tau, x) := (U_{(c\tau + x_0 - x_1, 0)} \Psi_\tau)(x) = \Psi_\tau(c\tau + x_0 - x_1, x)$$

Ψ_τ should be a solution of (1) and (3), so we get

$$\begin{aligned} i\hbar \frac{\partial}{\partial \tau} \Omega_A(\tau, x) &= H_0 \Omega_A - i\frac{\hbar}{2} g_1^+(x - x_1) g_1(x - x_1) \Omega_A \\ &\quad - i\frac{\hbar}{2} T g_2(x - x_2)^+ g_2(x - x_2) T^{-1} \Omega_A \end{aligned} \quad (9)$$

with $T = U_{(c\tau+x_0-x_1,0)}U_{(c\tau+x_0-x_2,0)}^{-1} = \exp\left(-\frac{i}{\hbar}(x_2-x_1)H_0\right)$. A solution of this equation has to be found satisfying the initial condition $\Omega_A(0, x) = \Psi_0(x_0 - x_1, x)$. The equation (9) is solved numerical with the proper time dynamics approximated by

$$\begin{aligned} \Omega_A(\tau + \Delta\tau) &\approx \\ &\exp\left(-\frac{\Delta\tau}{2}\frac{i}{\hbar}mc^2\gamma^0 - \frac{\Delta\tau}{2}\frac{1}{2}g_1^+(x-x_1)g_1(x-x_1)\right) \exp\left(-\frac{\Delta\tau}{2}\frac{i}{\hbar}\left(-i\hbar c\gamma^0\gamma^1\frac{\partial}{\partial x}\right)\right) \\ T \exp\left(-\Delta\tau\frac{1}{2}g_2^+(x-x_2)g_2(x-x_2)\right) T^{-1} \exp\left(-\frac{\Delta\tau}{2}\frac{i}{\hbar}\left(-i\hbar c\gamma^0\gamma^1\frac{\partial}{\partial x}\right)\right) \\ &\exp\left(-\frac{\Delta\tau}{2}\frac{i}{\hbar}mc^2\gamma^0 - \frac{\Delta\tau}{2}\frac{1}{2}g_1^+(x-x_1)g_1(x-x_1)\right) \Omega_A(\tau) \end{aligned}$$

with $T \approx \prod \exp\left(-\Delta\tau\frac{i}{\hbar}H_0\right)$.

We discretize the proper time and the space with steps $\Delta\tau$ and Δx ($c\Delta\tau = \Delta x$). The boundary conditions are walls at $x = -8 \text{ \AA}$ and $x = 8 \text{ \AA}$ in such a way that $\Omega_A(\tau, -8 \text{ \AA}) = \Omega_A(\tau, 8 \text{ \AA}) = 0$ for all τ .

All operators (including T) can be evaluated directly or are approximated by using the method of Wessels, Caspers, and Wiegel [17] or by using Wendroff's formula (see e.g. [18]).

For simulating the second part of the algorithm (after a first detection by detector D_1 at proper time τ_1), we define

$$\Omega_B^{(\tau_1)}(\tau, x) := (U_{(c\tau+x_0-x_2,0)}\Psi_\tau)(x) = \Psi_\tau(c\tau + x_0 - x_2, x)$$

with Ψ_τ being a solution of (1) and (3). We get

$$i\hbar\frac{\partial}{\partial\tau}\Omega_B^{(\tau_1)}(\tau, x) = H_0\Omega_B^{(\tau_1)}(\tau, x) - i\frac{\hbar}{2}g_2^+(x-x_2)g_2(x-x_2)\Omega_B^{(\tau_1)}(\tau, x) \quad (10)$$

We must solve this equation with the initial condition

$$\Omega_B^{(\tau_1)}(\tau_1, x) = \frac{T^{-1}g_1(x-x_1)\Omega_A(\tau_1, x)}{\sqrt{\int dx \Omega_A^+(\tau_1, x)g_1^+(x-x_1)g_1(x-x_1)\Omega_A(\tau_1, x)}} \quad (11)$$

The equation (10) with the initial condition (11) can be solved approximately in analogy to Section 4.1.

Knowing $\Omega_A(\tau, x)$ and $\Omega_B^{(\tau_1)}(\tau, x)$, we can calculate $P_{\infty,12}$ and $p_{12}(\tau_1, \tau_2)$. So we can calculate $\rho_0(t)$ and $T_{t,0}$.

We do the computation with proper time and space step $c\Delta\tau_B = \Delta x_B = 0.0006$. The value of τ_{CUT} depends on the particle momentum: $\tau_{CUT} = 31.5 \text{ \AA}/c$ ($p_0 = 0.25 mc$), $\tau_{CUT} = 17.5 \text{ \AA}/c$ ($p_0 = 0.5 mc$), $\tau_{CUT} = 13.5 \text{ \AA}/c$ ($p_0 = 0.75 mc$), $\tau_{CUT} = 11.5 \text{ \AA}/c$ ($1.0 mc \leq p_0 < 1.5 mc$), $\tau_{CUT} = 10.5 \text{ \AA}/c$ ($1.5 mc \leq p_0$).

Moreover, we do the computation with proper time and space step $c\Delta\tau_A = \Delta x_A = 0.001$. So the error in the expectation value $T_{t,0}$ can be approximated by

$$\text{error}(T_{t,0}) = \pm \frac{\Delta x_B}{\Delta x_A - \Delta x_B} |T_{t,0}(\Delta x_B) - T_{t,0}(\Delta x_A)| \quad (12)$$

The error in the probability $P_{\infty,12}$ is approximated by a similar formula:

$$\text{error}(P_{\infty,12}) = \pm \frac{\Delta x_B}{\Delta x_A - \Delta x_B} |P_{\infty,12}(\Delta x_B) - P_{\infty,12}(\Delta x_A)| \quad (13)$$

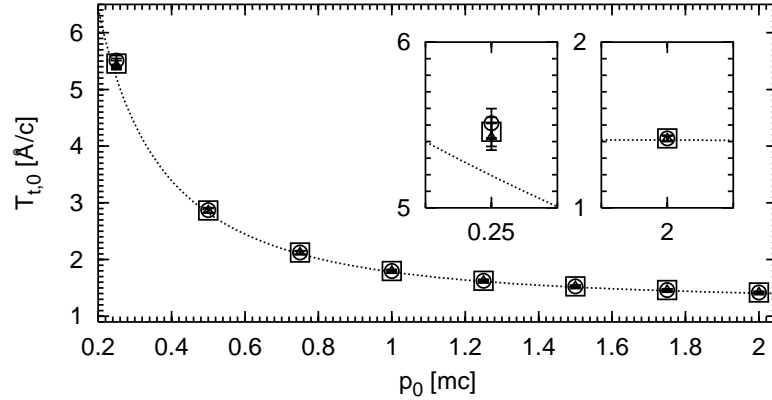


Figure 3. Mean traversal time $T_{t,0}$ versus particle momentum p_0 in the detectors' rest-frame K_0 , starting with different initial states : $\Psi_{0,P}$ (boxes with error bars), $\Psi_{0,N}$ (triangles with error bars), $\Psi_{0,P,N}$ (circles with error bars), other parameters see text; results from classical relativistic mechanics $t_{t,RM}$ (dotted line)

5.2. Results

We perform the simulation with different initial states and different particle momenta p_0 . We set $x_0 = -1.5 \text{ \AA}$. The detector parameters are $x_1 = 0 \text{ \AA}$, $\Delta x_1 = 0.5 \text{ \AA}$, $W_1 = 1 \times 10^{-3} mc^2$ and $x_2 = 1.26 \text{ \AA}$, $\Delta x_2 = 0.02 \text{ \AA}$, $W_2 = 1 \times 10^{-3} mc^2$.

Now, we are interested in the traversal time in the detectors' rest-frame K_0 . Figure 3 shows the expectation values for traversal time with different initial states and different particle momenta p_0 . The errors calculated by (12) are also plotted.

A first result is that we see nearly no dependence on the initial state.

In addition, the times which one obtains by using classical relativistic mechanics of a point-particle are plotted:

$$t_{t,RM} = \frac{x_2 - x_1}{c} \cdot \sqrt{1 + \frac{m^2 c^2}{p_0^2}}$$

There is a good agreement between the simulated results and those obtained by using classical relativistic mechanics. This agreement becomes more accurate with increasing particle momentum p_0 .

Figure 4 shows the probability densities ρ_0 for traversal time in the detectors' rest-frame K_0 with different initial states. The probability densities have a peak at the classical expected traversal time. Again, we see that there is nearly no difference if we start with the initial state $\Psi_{0,P}$ or $\Psi_{0,N}$. There are only small differences with the results obtained with the initial state $\Psi_{0,P,N}$.

Next, we examine the situation in a moving reference frame K_v . It moves with velocity v relative to K_0 . We calculate the traversal time in the framework of classical relativistic mechanics:

$$\tilde{t}_{t,RM} = \frac{1}{\sqrt{1 - \frac{v^2}{c^2}}} \cdot \left[t_{t,RM} - \frac{v}{c^2} (x_2 - x_1) \right]$$

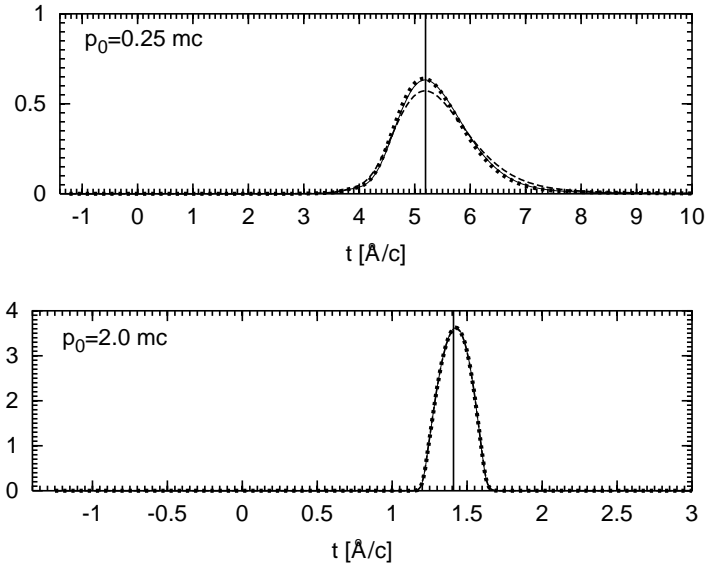


Figure 4. Probability densities ρ_0 for traversal time in the detectors' rest-frame K_0 , initial state: $\Psi_{0,P}$ (small solid line), $\Psi_{0,N}$ (big dotted line), $\Psi_{0,PN}$ (dashed line), particle momentum p_0 ; the vertical solid line indicates the traversal time given by classical relativistic mechanics

We get the same correlation between $t_{t,RM}$ and $\tilde{t}_{t,RM}$ in classical relativistic mechanics than the correlation between $T_{t,0}$ and $T_{t,v}$ in our formalism (see (8)). We get the same result than in the time-of-arrival case: the good agreement between our results and those obtained in classical relativistic mechanics exists in all reference frames.

Now, we want to examine how the results depend on the detector parameters. The particle momentum is fixed at $p_0 = 0.75 mc$ and the initial quantum state is $\Psi_{0,P}$.

We start by varying the parameters of the first detector D_1 . The parameters of the second detector D_2 are fixed at $\Delta x_2 = 0.02 \text{ \AA}$ and $W_2 = 1 \times 10^{-3} mc^2$.

First, we compute $P_{\infty,12}$ and the expectation value $T_{t,0}$ in K_0 for different detector widths Δx_1 while keeping $W_1 = 1 \times 10^{-3} mc^2$ fixed (see Figure 5a). We find out that it exists a range of detector width ($0.3 \text{ \AA} \lesssim \Delta x_1 \lesssim 1.0 \text{ \AA}$) for which the expectation value $T_{t,0}$ does not change in a significant way. But the probability for two detections $P_{\infty,12}$ increases with increasing detector width Δx_1 .

In the range $0.3 \text{ \AA} \lesssim \Delta x_1 \lesssim 1.0 \text{ \AA}$ the forms of the probability densities ρ_0 do not differ in a significant way. The peaks only become wider with increasing detector width Δx_1 . If the detector width is very small ($\Delta x_1 = 0.02 \text{ \AA}$), the wave function changes strongly through the detection by D_1 and so we get a qualitatively different probability density ρ_0 .

Now we fix $\Delta x_1 = 0.5 \text{ \AA}$ and vary W_1 (see Figure 5b). In the case of weakly intrusive detectors $W_1 \lesssim 5 \times 10^{-3} mc^2$, the expectation values $T_{t,0}$ do not differ in a significant way. For higher detectors, the expectation values $T_{t,0}$ increase a bit with increasing detector height W_1 . The probability $P_{\infty,12}$ increases with increasing W_1 , a fact one expects intuitively.

With increasing detector height W_1 , the peak of the probability densities ρ_0 is

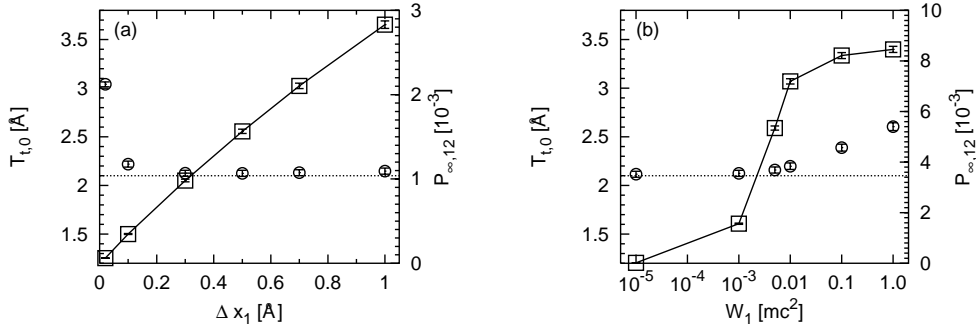


Figure 5. Mean traversal time $T_{t,0}$ (circles with error bars, left axis) and probability $P_{\infty,12}$ (boxes with error bars connected with a solid line, right axis); initial state $\Psi_{0,P}$ with $p_0 = 0.75mc$; detector D_2 : $\Delta x_2 = 0.02 \text{ \AA}$, $W_1 = 1 \times 10^{-3} mc^2$; the dotted line indicates the traversal time deduced from classical relativistic mechanics; (a) detector height $W_1 = 1 \times 10^{-3} mc^2$; (b) detector width $\Delta x_1 = 0.5 \text{ \AA}$

shifted to higher traversal times.

In the last part of this section, we fix the parameters of D_1 at $\Delta x_1 = 0.5 \text{ \AA}$ and $W_1 = 1 \times 10^{-3} mc^2$ and we vary the parameters Δx_2 and W_2 of detector D_2 . We examine the following pairs of detector parameter $\Delta x_2 = 0.02 \text{ \AA}/W_2 = 1 \times 10^{-3} mc^2$, $\Delta x_2 = 0.02 \text{ \AA}/W_2 = 1.0 mc^2$, $\Delta x_2 = 0.5 \text{ \AA}/W_2 = 1 \times 10^{-3} mc^2$, and $\Delta x_2 = 0.5 \text{ \AA}/W_2 = 1.0 mc^2$. We find that the resulting probability densities ρ_0 and expectation values $T_{t,0}$ are nearly the same in the first three cases. The only exception is the case of a very wide and “height” detector (last case). In that case, the mean traversal time $T_{t,0}$ is lower than in the other cases.

The probability $P_{\infty,12}$ grows significantly if one increases the detector width Δx_2 or the detector height W_2 . We get the same qualitative dependence of $P_{\infty,12}$ on the parameters of detector D_2 as on the parameters of detector D_1 .

Note that the following fact is true in the case of weakly intrusive detectors ($W_1 = W_2 = 1 \times 10^{-3} mc^2$): the dependence of $T_{t,0}$ on Δx_1 is “stronger” than the dependence on Δx_2 . The reason for this is clear: changing the width Δx_1 of the first detector D_1 change not only the first “detection-time” but also the form of the wave function after the first detection.

Summarizing, it exists a wide range of parameters of D_1 and D_2 for which the mean traversal time does not change significantly. Remember that the same result was found in the study of time-of-arrival.

6. Conclusion

In [6], we have proposed an extension of EEQT describing one spin $\frac{1}{2}$ -particle in a relativistic, covariant way.

In this paper, we have focused on applications of this formalism. We have calculated detection times of the particle in two-dimensional spacetime. The particle has moved freely except of the influence exerted on it by the detector(s).

As a first application, we have computed the time at which the particle arrives at a detector (“free time-of-arrival”). We have found out that there exists good agreement

between the expectation values of our simulation and the results obtained by using classical relativistic mechanics of a free point particle. Moreover, we have shown that this fact is independent of the reference frame: the agreement is equally good in all reference frames. We have considered the situation with different detectors. We have found out that the good agreement between the results of our algorithm and the results obtained by using classical relativistic mechanics is not limited to a special value of detector parameters. It is obtained for a wide range of detector parameters.

As a second application, we have examined the time difference between two detections of the particle by two detectors, one behind the other (“free traversal time”). Again, we have obtained good agreement between the simulated results and those obtained by classical relativistic mechanics in all reference frames. Moreover, we have shown that there again exist a wide range of detector parameters for which the mean traversal time does not change significantly.

Summarizing, we have found interesting and meaningful results in these applications of our relativistic extension of EEQT. So we think that our formalism will be also useful in future applications, for example in the case, in which the particle is submitted to the action of a potential barrier.

Acknowledgments

I would like to thank Ph. Blanchard for many helpful discussions and the critical reading of the manuscript.

References

- [1] Blanchard Ph and Jadczyk A 1993 *Phys. Lett. A* **175** 157-64
- [2] Blanchard Ph and Jadczyk A 1995 *Phys. Lett. A* **203** 260-6
- [3] Blanchard Ph and Jadczyk A 1995 *Ann. Phys.* **4** 583-99
- [4] Blanchard Ph, Jadczyk A and Ruschhaupt A 2000 *J. Mod. Optics* **47** 2247-63
- [5] Blanchard Ph and Jadczyk A 1996 *Found. Phys.* **26** 1669-81
- [6] Ruschhaupt A 2002 *Preprint* quant-ph/0204079
- [7] Muga J G, Sala R and Palao J P 1998 *Superlattices Microst.* **23** 833-42
- [8] Muga J G and Leavens C R 2000 *Phys. Rep.* **338** 353-438
- [9] Blanchard Ph and Jadczyk A 1996 *Helv. Phys. Acta* **69** 613-35
- [10] Hauge E H and Støvneng J A 1989 *Rev. Mod. Phys.* **61** 917-36
- [11] Landauer R and Martin Th 1994 *Rev. Mod. Phys.* **66** 217-28
- [12] Nimtz G and Heitmann W 1997 *Prog. Quant. Electron.* **21** 81-108
- [13] Chiao R Y and Steinberg A M 1997 *Prog. Optics* **37** 345-405
- [14] Palao J P, Muga J G, Brouard S and Jadczyk A 1997 *Phys. Lett. A* **233** 227-32
- [15] Ruschhaupt A 1998 *Phys. Lett. A* **250** 249-56
- [16] Ruschhaupt A 2000 *Decoherence: Theoretical, Experimental, and Conceptual Problems* LNP 538 ed Ph Blanchard et al. (Springer) pp. 259-69
- [17] Wessels P P F, Caspers W J and Wiegel F W 1999 *Europhys. Lett.* **46** 123-6
- [18] Mitchell A R and Griffiths D F 1980 *The Finite Difference Method in Partial Differential Equations* (John Wiley & Sons Ltd.)